

PHENIX photons and dileptons

 Takao Sakaguchi, for the PHENIX Collaboration^a
^a*Brookhaven National Laboratory, Physics Department*

Abstract

Electro-magnetic probes such as dileptons and photons are strong probes to investigate the thermodynamical state of the early stages of collisions since they leave the system unscathed. The PHENIX experiment has measured both photons and dileptons in p+p, d+Au and Au+Au collisions. An excess of dilepton yield over the expected hadronic contribution is seen in 0.2–0.8 GeV/ c^2 in Au+Au collisions, which is prominent in lower p_T and most central. Direct photons are measured through their internal conversion to electron pairs. We saw a large enhancement in Au+Au collisions over p+p yield scaled by the number of binary collisions. It turned out from the latest results on d+Au collisions that this enhancement is not explainable by a nuclear effect.

Keywords:

1. Introduction

Many intriguing phenomena have been observed at RHIC where a hot and dense matter is expected to be created. The large suppression of the yield of the single hadrons at high transverse momentum (p_T) suggested that the matter is so dense to stem fast partons with large Q^2 emerged from the very early stage in the medium [1]. The large elliptic flow of particles and its scaling in terms of kinetic energy of the particles suggests that the system is locally in equilibrium at as early as 0.3 fm/c. Although the hadronic probes already exhibited many interesting phenomena, since they are suffered from strong interactions in later stages to some extent, observation of more direct and penetrating probes have been desired.

Electro-magnetic probes such as photons or dileptons are ideal in this sense, since they interact with medium or other particles only electro-magnetically, once produced [2]. Therefore, these probes are of interest already from the beginning of the history of the heavy ion collisions. At the leading order, the production processes of photons are annihilation ($q\bar{q} \rightarrow \gamma g$) and Compton scattering ($qg \rightarrow \gamma q$). Their yields are proportional to $\alpha\alpha_s$, which are ~ 40 times lower than the ones from strong interaction. The dilepton production is mainly from annihilation of quark and anti-quark ($q\bar{q} \rightarrow \gamma^*$), and the yield is proportional to α^2 . Except for some difference in production processes, photons and dileptons can be treated as same observables. A theoretical calculation tells that photons and dileptons share similar emission sources [3]. Fig 1 shows a mapping of photons and dileptons in one coordinate.

PHENIX has measured dileptons and photons since the RHIC has started its running in 2000. In this paper, we show the most recent results on dileptons and photons in p+p, d+Au and Au+Au collisions at $\sqrt{s_{NN}}=200$ GeV.

2. Dilepton analysis

The PHENIX detector has a capability of measuring momentum of charged particles with high accuracy and of identifying electrons with high efficiency and strong rejection power of hadrons [4]. In measuring dileptons, we have

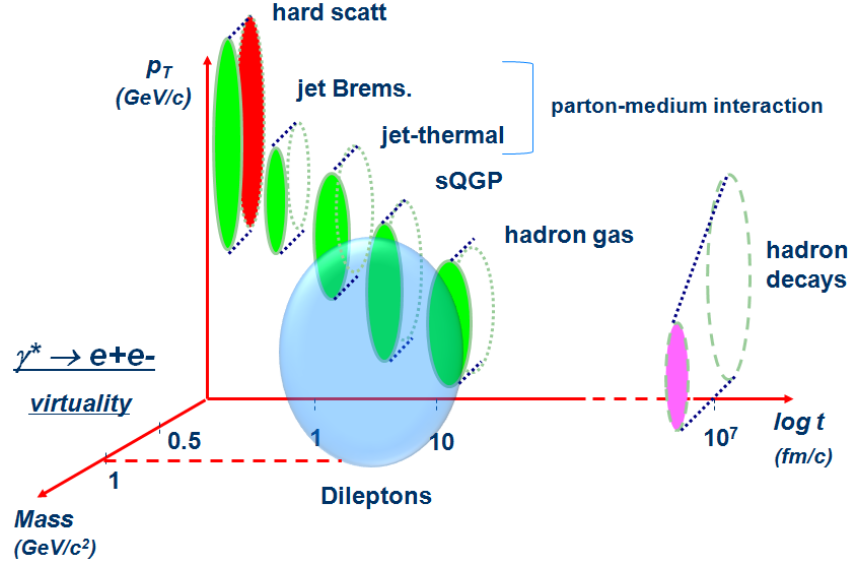


Figure 1: Photons and dileptons in one coordinate with three degrees of freedom.

a huge combinatorial background e^+e^- arising from random combination of electrons from photons converted at beam pipe, Dalitz decays of π^0 or η . We constructed combinatorial background by combining electrons or positrons from different events, and subtracted them from foreground mass distributions.

The subtracted distributions still include unphysical correlated pairs from back-to-back jets. We estimated the contribution using PYTHIA event generator followed by a detector simulation, and subtracted it off from the invariant mass distribution. The signal to background ratio is $\sim 10^{-2}$ in total. The resulting distribution is corrected for efficiencies of single electrons, and compared to various hadronic contributions.

3. Low mass and low p_T dileptons in Au+Au collisions

Fig 2(a) shows the invariant mass distribution of electron pairs measured in Au+Au collisions at $\sqrt{s_{NN}}=200\text{GeV}$ [5]. The data is compared with electron pairs from various hadronic sources calculated using a Monte Carlo and filtered by the PHENIX acceptance. A large excess is seen in 0.2-0.8 GeV/c^2 in Minimum bias Au+Au collisions. In order to study this excess in detail, we divided the data set into various p_T , mass and centrality bins. Fig. 2(b) and (c) show the mass spectra in various p_T and centrality bins, respectively. The excess dies out at higher p_T and lower centralities, which suggests that the excess is contributed from a thermal source. We made summary plots for the detail studies as shown in Fig. 3(a) and (b). As we already saw in the invariant mass distributions, the yield of excess region increases as collisions become more central. The slope parameters are low for low $m_T - m_0$ and high for high $m_T - m_0$, implying that the local slopes are roughly proportional to the energy of photons emitted. This is another evidence of that they are from thermal sources.

4. Low mass and high p_T dileptons in Au+Au and p+p

Turning the region of interest to higher p_T , where $p_T \gg M$, the yield of dileptons are considered to be dominated by internal conversion of real photons as depicted in Fig 4(a). Taking this advantage, we performed direct photon measurement through dilepton measurement [6]. The invariant mass distribution of Dalitz decay of π^0 , η and direct

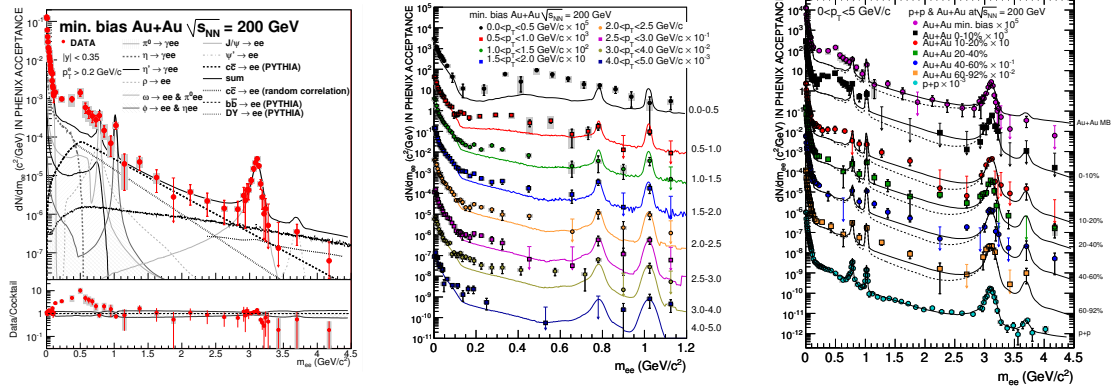


Figure 2: (a, left) Invariant mass distributions in Minimum bias Au+Au events with hadronic cocktail calculation, and the ones in (b, middle) various p_T regions and in (c, right) centrality classes.

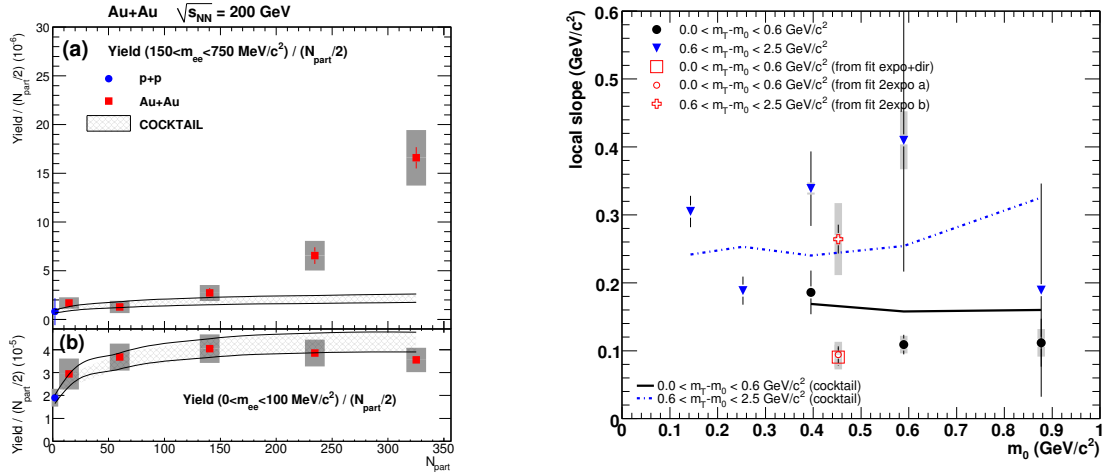


Figure 3: (a, left) Yield and (b, right) slope parameters of dileptons in low mass and low p_T region. For slope parameters, solid points are calculated from truncated means of the mass distributions, while open points are from exponential fits to the distributions.

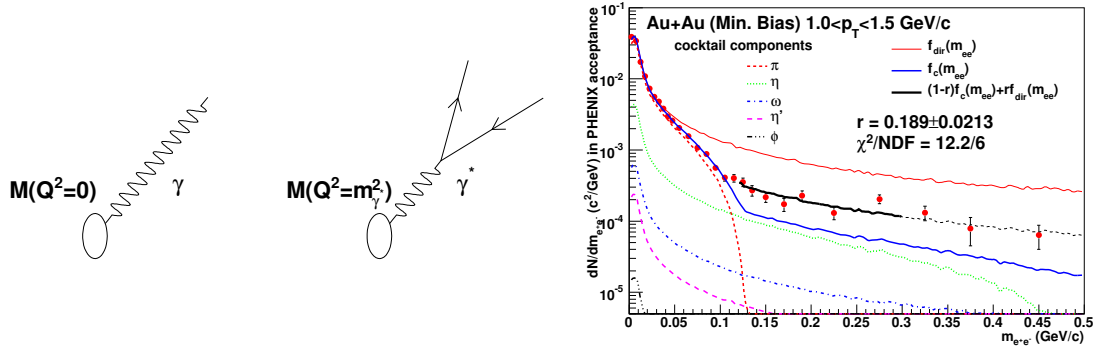


Figure 4: (a, left) Diagram of real photons and internal conversion of photons. (b, right) Fit to data with direct photon and hadronic cocktail distributions.

photons can be calculated using Kroll-Wada formula as shown below.

$$\frac{1}{N_\gamma} \frac{dN_{ee}}{dm_{ee}} = \frac{2\alpha}{3\pi} \sqrt{1 - \frac{4m_e^2}{m_{ee}^2}} \left(1 + \frac{2m_e^2}{m_{ee}^2}\right) \frac{1}{m_{ee}} |F(m_{ee}^2)|^2 \left(1 - \frac{m_{ee}^2}{M^2}\right)^3$$

Then, the real invariant mass distribution is fitted with a function of:

$$F = (1 - r)f_c + rf_d$$

where f_c is the cocktail calculation, f_d is the mass distribution for direct photons, and r is the free parameter in the fit. Using Kroll-Wada formula, r is converted to direct photon to inclusive photon ratio as follows:

$$r = \frac{\gamma_{dir}^*(m_{ee} > 0.15)}{\gamma_{inc}^*(m_{ee} > 0.15)} \propto \frac{\gamma_{dir}^*(m_{ee} \approx 0)}{\gamma_{inc}^*(m_{ee} \approx 0)} = \frac{\gamma_{dir}}{\gamma_{inc}} \equiv r_\gamma$$

Once r_γ is obtained, the invariant yield of direct photons are calculated as $\gamma_{inc} \times r_\gamma$. The procedure demonstrated in Fig 4(b) is for $1.0 < p_T < 1.5$ GeV/c. The dotted lines show the contributions from various hadrons, the solid blue is the sum of these contributions, and the solid red line show the distribution by direct photons converted internally. The r value is determined by the fit to the data. The error of the fit corresponds to the statistical error. We applied the procedure for various p_T s and centralities in p+p and Au+Au collisions, and obtained the p_T spectra as shown in Fig 5(a). The result is obtained from 810 million Minimum bias Au+Au events collected in RHIC Year-4 run, and

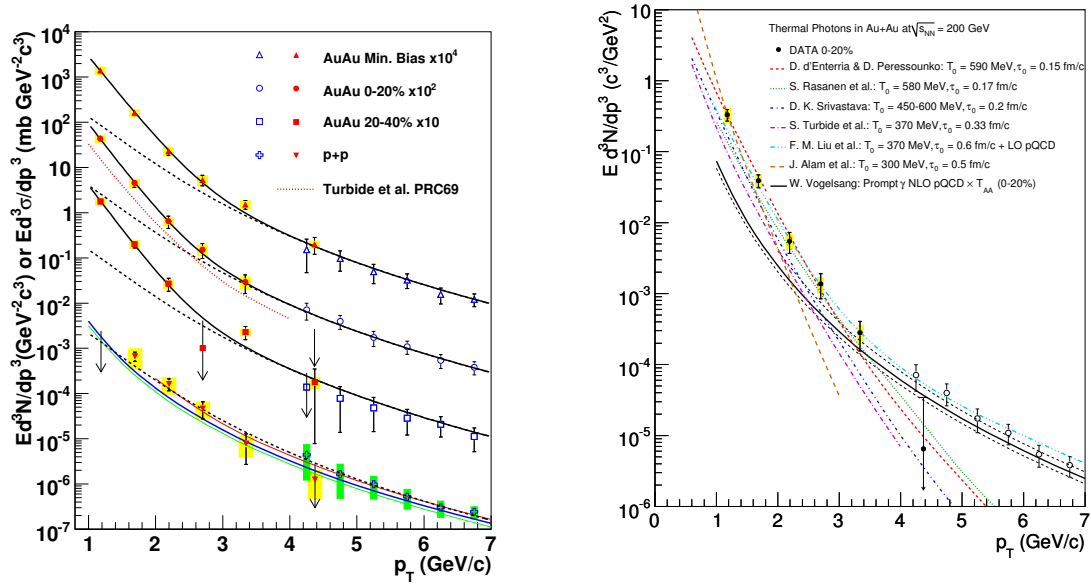


Figure 5: (a, left) Direct photon yields in p+p and Au+Au collisions. (b, right) Comparison of the yield in 0-20 % Au+Au collisions with various theoretical models.

1.5 billion minimum bias events and 270 million high p_T single electron trigger events collected in RHIC Year-5 p+p run. The distributions are for 0-20 %, 20-40 % centrality and Minimum Bias collisions in case of Au+Au collisions. The distributions were then fitted with the p+p fit plus exponential function. We obtain slopes and dN/dy for three centralities as shown in Table 4. There are many models in the market that have a wide range of initial temperatures and thermalization times. Fig 5(b) shows the comparison of the data with the models. Since the initial temperature and thermalization time are highly correlated, the comparison of data and models does not help constraining two parameters to definite numbers.

Table 1: dN/dy and slopes of direct photon p_T distributions obtained from the fit to the data with the p+p fit plus exponential function.

Centrality	dN/dy ($p_T > 1$ GeV/c)	Slope (MeV)	χ^2/DOF
0-20 %	$1.50 \pm 0.23 \pm 0.35$	$221 \pm 19 \pm 19$	4.7/4
20-40 %	$0.65 \pm 0.08 \pm 0.15$	$217 \pm 18 \pm 16$	5.0/4
MinBias	$0.49 \pm 0.05 \pm 0.11$	$233 \pm 14 \pm 19$	3.2/4

5. Low mass and high p_T dileptons in d+Au

It has been a question whether or not the excess is purely from the source that only exists in Au+Au collisions. A possible effect that increases the the yield in nucleus collisions is k_T broadening, or so-called Cronin effect. In order to quantify the effect, we analyzed d+Au data from RHIC Year-8 run with the same procedure. Fig. 6(a) shows the invariant mass distribution in d+Au collisions for the lowest p_T where the direct photon yield is significant. After repeating over p_T bins, we obtained the r_γ as a function of p_T . Fig 6(b) shows the r_γ in various collision systems. The lines show the ratios calculated using the direct photon contributions estimated by NLO pQCD prediction scaled by the number of binary collisions (N_{coll}). Three lines show the predictions with three mass scales ($\mu = p_T/2, p_T, 2p_T$). The p+p ratio is very close to the NLO pQCD prediction, while Au+Au data largely deviates in low p_T from the prediction. The d+Au data shows a moderate excess, but the excess is not as much as the one in Au+Au collisions. From the ratios obtained, we calculated the direct photon spectra, again following the procedure explained previously.

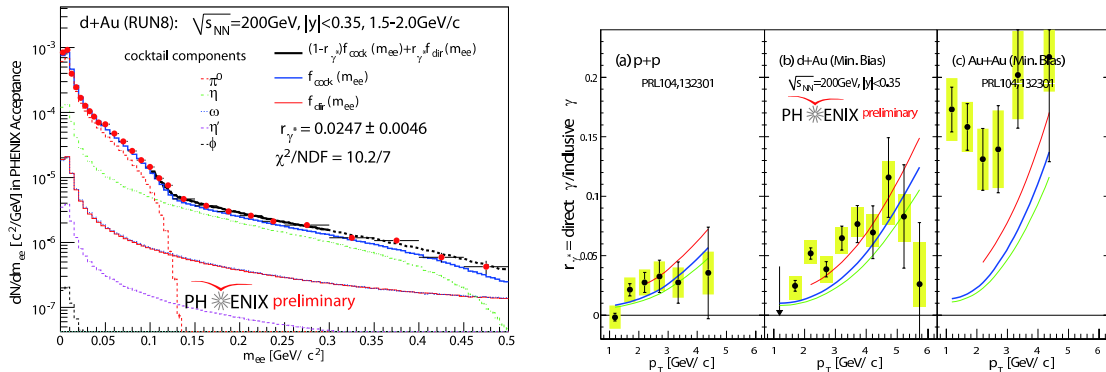


Figure 6: (a, left) Invariant mass distribution together with the calculation for hadronic cocktail and direct photons. The procedure to obtain r' is described in analysis section. (b, right) Ratios of γ_{dir} to γ_{inc} for p+p, d+Au and Au+Au collisions.

Fig 7(a) shows the direct photon spectra for d+Au Minimum bias events, together with the real photon result from RHIC Year-3 run. A comparison is made with direct photon spectra from p+p collisions scaled by N_{coll} . Fig. 7(b) shows a comparison of data with NLO pQCD calculation scaled by N_{coll} . In both cases, the yield in d+Au collisions are higher than the one expected from p+p yield, suggesting that the nuclear effect is seen in d+Au collisions.

The ultimate interest in the series of the direct photon measurements is whether or not the excess seen in Au+Au collisions can be explained by cold nuclear effect (Cronin effect). In order to evaluate this, we compared the Au+Au yield with the d+Au yield scaled by the difference of N_{coll} as shown in Fig 8(a). As seen in the plot, the Au+Au yield is higher than the one in d+Au in $p_T < 2.5$ GeV/c, which is close to what is expected in a literature [3]. When we divide Au+Au by N_{coll} -scaled d+Au data, we clearly see the existence of an additional effect in Au+Au collisions (Fig. 8(b)).

Since both statistical and systematic uncertainties are still very large in d+Au measurement, it is hard to exhibit a concrete quantitative conclusion. However, in order to visually improve the result, we tried to parameterize the d+Au points by using a fit function. Fig 9(a) shows a fit to the d+Au points and Fig 9(b) shows the fit scaled by N_{coll} and Au+Au points. The excess in Au+Au for $p_T < 2.5$ GeV/c still looks to be definite compared to the yield in d+Au,

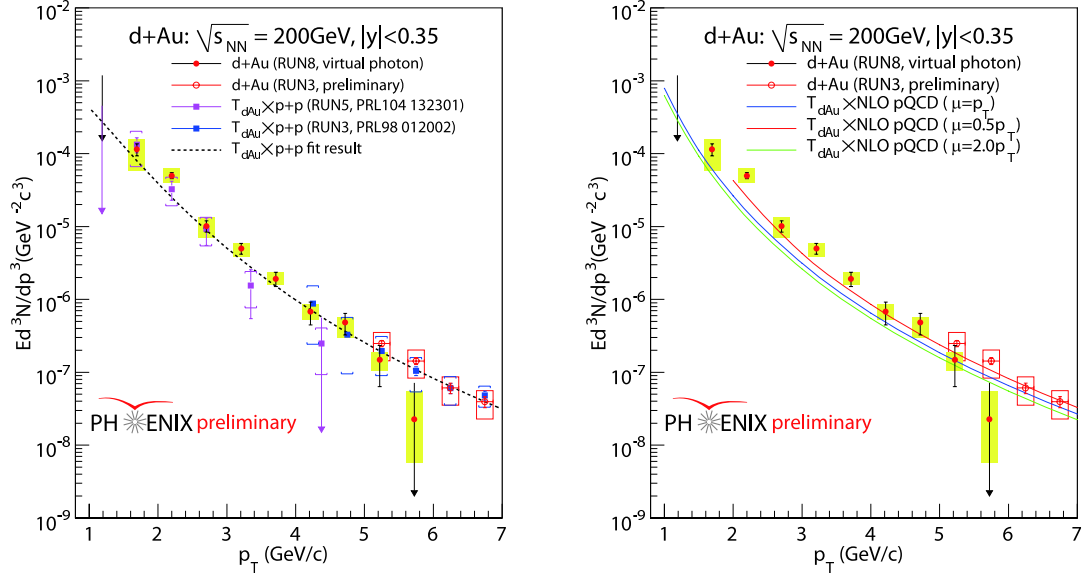


Figure 7: (a, left) Direct photon yield in d+Au collisions from this analysis together with Run3 real photon result and p+p yield scaled by N_{coll} . (b, right) The same data with NLO pQCD calculation, instead of p+p yield.

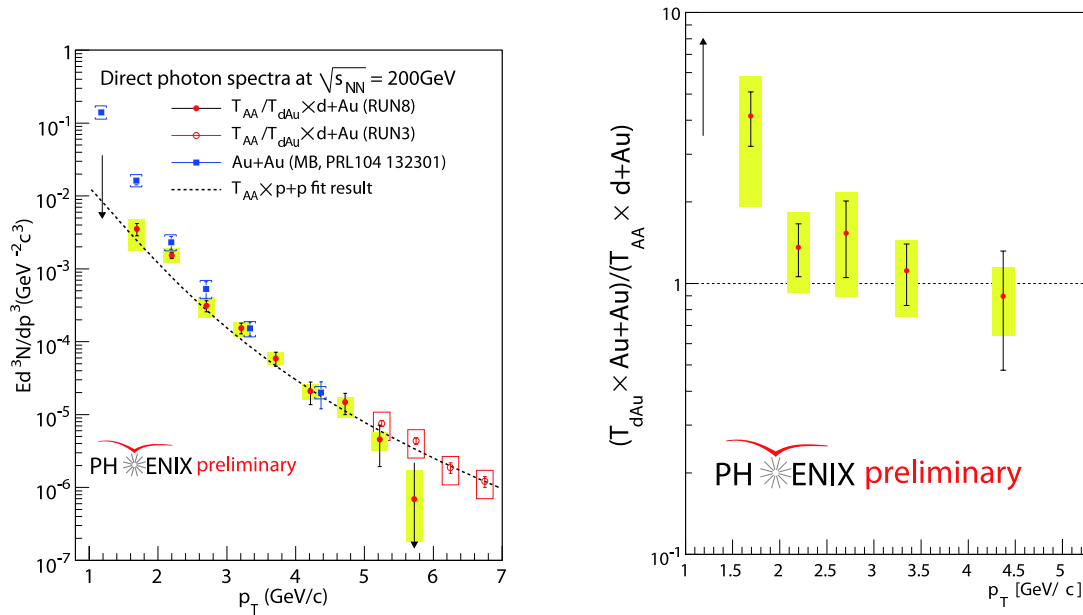


Figure 8: (a, left) Direct photon yields in Au+Au and d+Au collisions scaled by the difference of N_{coll} in both collision systems. (b, right) Ratio of Au+Au yield to d+Au yield scaled by N_{coll} .

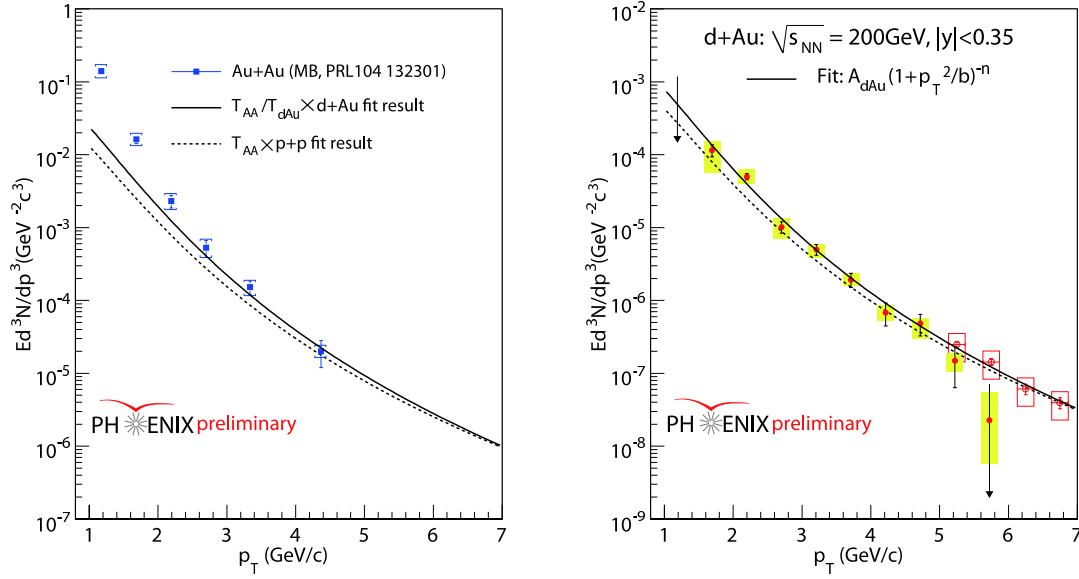


Figure 9: (a, left) Fit to the d+Au invariant yield, and (b, right) comparison of the fit and Au+Au yield.

implying that the excess is caused by a source created in hot dense medium.

6. Toward better measurement of dileptons

The statistical uncertainty and a part of systematic uncertainty in dilepton measurement are governed by the background arising from random combinations of electrons from photons converted at beam pipe and Dalitz decay of π^0 and η . If we could tag and remove such electrons from foreground electron pair measurement, the errors would be reduced significantly.

We developed a hadron blind detector (HBD) to realize this tagging. The detector is windowless Čerenkov type detector with CF₄ gas in its radiator. We operate the detector in magnetic field free region in order to look for an opening angle of electron pairs. The principle of operation is following; if we see a cluster that has charge corresponding to the number of photo-electrons for single electrons, we keep the track associated with the cluster. If we see a cluster with double of the number of the photon-electrons, we reject the track associated with the cluster, assuming that this is contributed by two electrons, which are likely by photon conversion or Dalitz decay. The detail of the detector description and its performance can be found in [7]. Fig. 10 shows the invariant mass distributions with and without using HBD information from Year-9 p+p run at $\sqrt{s}=500\text{GeV}$. The signal to background ratios in ϕ , ω and ρ meson region are significantly improved after applying a charge cut in HBD. We are planning to also apply the charge cut in HBD in Au+Au collisions in RHIC Year-10 run data. It is essential in Au+Au collisions because the particle multiplicity is much higher than that in d+Au or p+p.

7. Summary

Electro-magnetic probes such as dileptons and photons are strong probes to investigate the thermodynamical state of the early stages of collisions since they leave the system unscathed. The PHENIX experiment has measured both photons and dileptons in p+p, d+Au and Au+Au collisions. An excess of dilepton yield over the expected hadronic contribution is seen in 0.2-0.8 GeV/c² in Au+Au collisions, which is prominent in lower p_T and most central. The invariant slopes are low for low $m_T - m_0$ and high for high $m_T - m_0$, implying that the local slopes are roughly

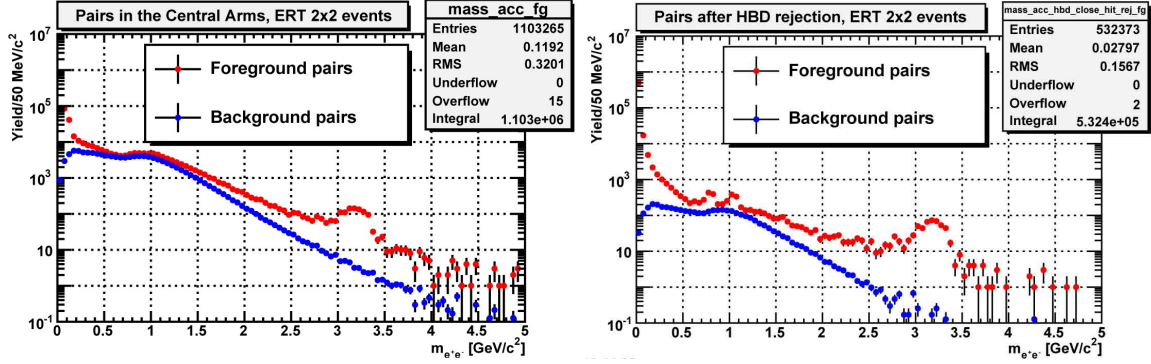


Figure 10: Dilepton invariant mass spectra (a, left) without HBD matching and (b, right) with HBD matching and a charge cut.

proportional to the energy of photons emitted. Direct photons are measured through their internal conversion to electron pairs. We saw a large enhancement in Au+Au collisions over p+p yield scaled by the number of binary collisions. It turned out from the latest results on d+Au collisions that this enhancement is not explainable by a nuclear effect.

References

- [1] K. Adcox *et al.* [PHENIX Collaboration], Nucl. Phys. A **757**, 184 (2005) [arXiv:nucl-ex/0410003].
- [2] P. Stankus, Ann. Rev. Nucl. Part. Sci. **55**, 517 (2005).
- [3] S. Turbide, R. Rapp and C. Gale, Phys. Rev. C **69**, 014903 (2004) [arXiv:hep-ph/0308085].
- [4] K. Adcox *et al.* [PHENIX Collaboration], Nucl. Instrum. Meth. A **499**, 469 (2003).
- [5] A. Adare *et al.* [PHENIX Collaboration], Phys. Rev. C **81**, 034911 (2010) [arXiv:0912.0244 [nucl-ex]].
- [6] A. Adare *et al.* [PHENIX Collaboration], Phys. Rev. Lett. **104**, 132301 (2010) [arXiv:0804.4168 [nucl-ex]].
- [7] M. Makek (PHENIX coll.), this proceedings.



Available online at www.sciencedirect.com



Procedia Computer Science 00 (2011) 1–1

**Procedia Computer
Science**

Abstract

Keywords:

1.